World Journal of Radiology

Online Submissions: http://www.wjgnet.com/esps/
bpgoffice@wjgnet.com
doi:10.4329/wjr.v5.i11.411

World J Radiol 2013 November 28; 5(11): 411-420
ISSN 1949-8470 (online)

ORIGINAL ARTICLE

Magnetically-coated silica nanospheres for dual-mode imaging at low ultrasound frequency

Fernanda Chiriacò, Giulia Soloperto, Antonio Greco, Francesco Conversano, Andrea Ragusa, Luca Menichetti, Sergio Casciaro

Fernanda Chiriacò, Giulia Soloperto, Antonio Greco, Francesco Conversano, Sergio Casciaro, Consiglio Nazionale delle Ricerche, Istituto di Fisiologia Clinica (CNR-IFC) c/o Campus Ecotekne, *via* per Monteroni, 73100 Lecce, Italy
Andrea Ragusa, National Research Council, Istituto di Nanoscienze, 73100 Lecce, Italy
Luca Menichetti, National Research Council, Institute of Clinical Physiology, 56100 Pisa, Italy
Author contributions: All the authors were involved in designing the study and writing the manuscript; Greco A performed the ultrasound experiments and data acquisition; Conversano F, Soloperto G did the data analysis and contributed to the paper drafting; Chiriacò F was involved in writing and editing the manuscript; Menichetti L, Ragusa A synthetized the dual mode nanoparticles and provided the scanning electron microscopy characterization; Casciaro S conceived and co-ordinated the study.
Supported by Italian Ministry of Instruction and Research, No. DM18604-Bando Laboratori-DD MIUR 14.5.2005 n.602/Ric/2005; by FESR PO Apulia Region 2007-2013-Action 1.2.4, No. 3Q5AX31; and by the Progetto Bandiera NANOMAX ENCODER
Correspondence to: Dr. Sergio Casciaro, Consiglio Nazionale delle Ricerche, Istituto di Fisiologia Clinica (CNR-IFC) c/o Campus Ecotekne, *via* per Monteroni, 73100 Lecce, Italy. sergio.casciaro@cnr.it
Telephone: +39-832-422310 Fax: +39-832-422341
Received: June 28, 2013 Revised: September 6, 2013
Accepted: October 18, 2013
Published online: November 28, 2013

Abstract

AIM: To experimentally investigate the acoustical behavior of different dual-mode nanosized contrast agents (NPCAs) for echographic medical imaging at low ultrasound (US) frequency.

METHODS: We synthesized three different nanosized structures: (1) Pure silica nanospheres (SiNSs); (2) FePt-iron oxide (FePt-IO)-coated SiNSs; and (3) IO-coated SiNSs, employing three different diameter of SiNS-core (160, 330 and 660 nm). Tissue mimicking phantoms made of agarose gel solution containing 5 mg of different NPCAs in 2 mL-Eppendorf tubes, were insonified by a commercial echographic system at three different low US pulse values (2.5, 3.5 and 4.5 MHz). The raw radiofrequency signal, backscattered from each considered NPCA containing sample, has been processed in order to calculate the US average backscatter intensity and compare the acoustic behavior of the different NPCA types.

RESULTS: The highest US contrast was exhibited by pure SiNSs; FePt-IO-coated SiNSs acoustical behavior followed a similar trend of pure SiNSs with a slight difference in terms of brightness values. The acoustic response of the examined NPCAs resulted function of both SiNS diameter and US frequency. Specifically, higher US frequencies determined higher value of the backscatter for a given SiNS diameter. Frequency-dependent enhancement was marked for pure SiNSs and became less remarkable for FePt-IO-coated SiNSs, whereas IO-coated SiNSs resulted almost unaffected by such frequency variations. Pure and FePt-IO-coated SiNSs evidenced an image backscatter increasing with the diameter up to 330 nm. Conversely, among the types of NPCA tested, IO-coated SiNSs showed the lowest acoustical response for each synthesized diameter and employed US frequency, although a diameter-dependent raising trend was evidenced.

CONCLUSION: The US characterization of magnetically covered SiNS shows that FePt-IO, rather than IO, was the best magnetic coating for realizing NPCAs suitable for dual mode imaging of deep organs, combining US and magnetic resonance imaging.

Key words: Ultrasound; Magnetic resonance; Nanocomposite; Dual-mode Imaging; Contrast agent; Diagnostic imaging

Core tip: In this work we investigated the acoustic response of novel dual-mode nanoparticle contrast agents, detectable through both ultrasound (US) and magnetic resonance imaging (MRI), made of silica nanospheres (SiNSs) of different diameters coated with superparamagnetic nanoparticles [iron-oxide (IO) or FePt-IO nanocrystals]. Magnetically-coated SiNSs were insonified with US pulses in the lower diagnostic range (2.5-4.5 MHz), which are commonly employed for the imaging of deep organs, and the results were compared with those of pure SiNSs. The US characterization of these nanocomposites shows that FePt-IO, rather than IO, was the best magnetic coating for realizing nano-sized contrast agents suitable for dual mode imaging of deep targets, combining US and MRI techniques.

Chiriacò F, Soloperto G, Greco A, Conversano F, Ragusa A, Menichetti L, Casciaro S. Magnetically-coated silica nanospheres for dual-mode imaging at low ultrasound frequency. *World J Radiol* 2013; 5(11): 411-420 Available from: URL: http://www.wjgnet.com/1949-8470/full/v5/i11/411.htm DOI: http://dx.doi.org/10.4329/wjr.v5.i11.411

INTRODUCTION

In medical practice and research, imaging is now playing a key role in the diagnosis and treatment of several disease, especially cancers. To date, various imaging methods are available for the assessment of pathophysiological changes at the molecular level. In addition to nuclear imaging modalities such as positron emission tomography and single photon emission computed tomography, conventional radiological modalities, such as computed tomography and magnetic resonance imaging (MRI), as well as ultrasound (US) imaging have been used for molecular imaging[1,2].

Each imaging modality has certain advantages as well as limitations. As different imaging tools are more complementary than competitive, multimodal imaging methods will be a powerful approach to improve the imaging quality. For instance, ultrasound is a real-time, non-ionizing, inexpensive, and widely available imaging modality with excellent detection depth, but it has poor tissue discrimination ability[3,4]. On the other hand MRI is a noninvasive imaging technique with exquisite soft tissue contrast and multi-planar imaging characteristics, but with a relatively long imaging time and the inability to provide real-time images[5]. Therefore, the two imaging modalities can potentially compensate the weakness of the other when integrated[6-8]. Specifically, the development of a novel class of dual-mode contrast agents, effectively providing the dual option of detection through US and MRI, would significantly improve currently adopted strategies for clinical diagnosis. In facts, given the complete absence of ionizing radiation and the considerable cost reduction for society, US could be used for initial tumor localization, and whereas a more accurate high-resolution tumor segmentation were necessary, MRI would be employed for a second-level investigation, with a single contrast agent injection.

The feasibility of US/MRI dual-modalities has been successfully demonstrated. Some studies indicated that US/MRI systems could provide benefits to better classify tissue/tumor and additionally provide complementary vascular information[9,10].

The US/MRI dual-mode contrast agents are mostly based on the existing US contrast media[1]. According to previous studies, microbubbles and nanobubbles for US imaging could encapsulate or absorb MRI contrast agents to achieve MRI/US dual-imaging[11-13].

The main drawback of such contrast agents (CAs), as studied by several research group, is represented by their unstable behavior and short life time[14,15]. In order to overcome such limitations, engineered solid microstructures are under investigation pursuing their safe implementation as CAs for different imaging modalities[16-19]. In particular, studies on magnetic and superparamagnetic nanoparticle contrast agents (NPCAs) for MRI, like ferrum-platinum (FePt) and iron-oxide (IO) nanocrystals, have been conducted, focusing the efforts on superficial functionalization of this NPCAs for multimodal molecular imaging, targeted cancer therapy and drug delivery[20-25]. Nanocomposite contrast agents have several potential advantages as their optical and magnetic properties can be tailored through the engineering of their composition, structure, size and shape[26]. In addition, the surface of these nanocomposites can be easily functionalized with a wide variety of biomolecules and could be adjusted for the target recognition of specific tissue/organ (*e.g.*, cancer tissues) improving *in vivo* detection and enhancing targeting efficiency[24-33].

Silica-based designs are popular in the literature both as shell coatings and as nanoparticle (NP) matrices for the development of non-invasive and ionizing radiation-free medical diagnostic techniques like ultrasonography and MRI[34-37]. In fact, silica offers a number of attractive features. Firstly, silica NPCAs can be synthetized in order to obtain specific dimensions, superficial pattern, particular blood circulation times, clearance pathways, and multivalent binding[34]. Moreover, these NPs are effectively "transparent" since they do not absorb light in the near-infrared (NIR), visible, and ultraviolet regions or interfere with magnetic fields[35]. In addition, silica NPs are inexpensive, easy to prepare, relatively chemically inert, biocompatible, and water dispersible[34].

In this context, our research group demonstrated the suitability of silica nanospheres (SiNSs) as NPCAs for ultrasound at conventional diagnostic US frequencies (7.5 and 10 MHz)[38-41]. Moreover we recently documented

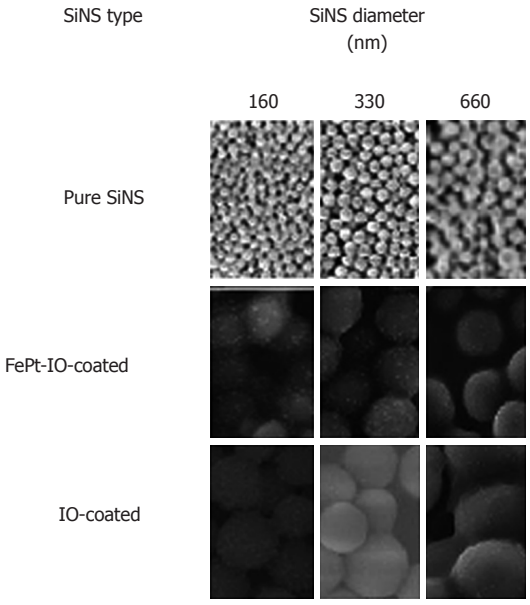

Figure 1 Overview of typical scanning electron microscopy images for each prepared nanoparticle contrast agents sample. Scale bars in the first row of pictures are 1 mm in 160 nm SiNS diameter, 3 mm in 330 nm SiNS diameter, and 5 mm in 660 nm SiNS diameter. SiNSs: Silica nanospheres; Pure: Uncoated SiNSs; FePt-IO: Ferrum platinum-iron oxide; IO: Iron oxide.

the potential of novel NPCAs based on SiNSs and coated with superparamagnetic NPs made of either IO or FePt-IO nanocrystal, for dual-mode imaging combining US and MRI imaging[38,42]. In particular, we documented the MRI detectability of magnetically-coated SiNSs, together with a good US contrast enhancement obtained at a value of US frequency (10 MHz) usually employed in clinical routine for imaging of superficial organs[38].

The frequency of ultrasound is crucial depending on the anatomical site being investigated. In general, high frequency pulses produce higher quality images but cannot penetrate very far into the body[43]. Conversely, low-frequency waves offer images of lower resolution but allow imaging of deeper structures, due to their lower degree of attenuation. Hence, high-frequency probes, between 7.5 and 10 MHz, are used to scan superficial structures such as vessels, nerves, and tendons whereas low-frequency probes, up to 4.5 MHz, are useful to scanning deeper structures such as the heart, abdomen and lungs.

The aim of the present work is to investigate the acoustic response of pure, FePt-IO- and IO-coated SiNSs, with three different SiNS diameters (160, 330 and 660 nm), to US pulses having frequencies in the lower diagnostic range (2.5-4.5 MHz), in order to explore the potentiality of this bimodal NPCAs for imaging of deep organs.

MATERIALS AND METHODS

NPCA synthesis

SiNSs were synthesized by a modified Stöber method[44], with a diameter of 160, 330, and 660 nm (mass density: 2.2 g/cm^3). The as-synthesized SiNSs were functionalized with aminopropyltriethoxysilane (APS) in order to replace the hydroxyl groups on their surface with amino groups for subsequent conjugation to the carboxy-functionalized magnetic nanocrystals.

Superparamagnetic IO nanocrystals (spherical; 15 nm in diameter; mass density: 5 g/cm^3) were prepared by a seeded-growth method as previously reported by Sun *et al*[45]. Heterodimeric FePt-IO nanocrystals, (asymmetric hetero-structured with a FePt magnetic domain of 5 nm in diameter and an iron oxide domain of 12 nm in diameter; mass density: 8.3 g/cm^3), have also been prepared as described by Figuerola *et al*[46].

The as-synthesized nanocrystals were prepared in organic solvents and transferred into aqueous medium by intercalating with poly(maleic anhydride- alt -1-octadecene) and adding a triamine, which yielded water-soluble NPs with an outer shell made of several carboxylic groups[47,48]. Direct addition of the solution with anhydride-coated magnetic nanocrystals to a suspension of APS-functionalized silica SiNSs led to the attachment of only a few nanocrystals through formation of amide bonds between the amino-functionalized SiNSs and the anhydride-functionalized nanocrystals.

Successful conjugation between the two types of NPs was confirmed performing the characterization of the as-synthesized nanocomposites with established techniques, such as dinamic light scattering, zeta-potential measurements, transmission electron microscopy and scanning electron microscopy (SEM).

In Figure 1, SEM images are reported for each SiNS diameter and type. Details on synthesis procedures of NPs were provided in our earlier paper[38].

Sample preparation

The *in vitro* study was conducted by investigating the echographic signal enhancement produced by 5 mg of pure and composite SiNSs with three different dimensions (160, 330 and 660 nm) dispersed in 1 mL of pure agarose gel, employed as tissue mimicking material.

The number of investigated phantoms, synthesized in Eppendorf tube (1 cm diameter tube for a total 2 mL volume), could be detailed as follows: (1) 3 of pure SiNS containing samples (one per each examined SiNS diameter); (2) 3 IO-coated SiNS containing samples (one per each examined SiNS diameter); and (3) 3 FePt-IO-coated SiNS containing samples (one per each examined SiNS diameter).

Each Eppendorf tube was first filled with 750 μL of pure agarose gel on the bottom, then 1 mL of gel containing 5 mg of a specific NPCA was added[40]. A further Eppendorf tube was filled with 1.75 mL of pure agarose gel and used as a control.

Each sample was analyzed in triplicate; therefore, a total of 28 Eppendorf tubes were prepared, one per each combination of SiNS diameter and type of coating.

The size of a magnetically coated SiNS will refer to the size of the uncoated SiNS, *i.e.*, 330 nm Si@IO indicated a SiNS with a 330 nm diameter coated with IO.

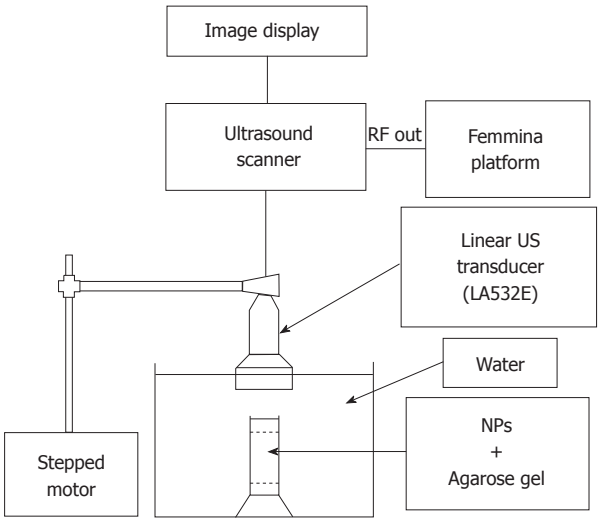

Figure 2 Scheme of the employed ultrasound acquisition system. The image display and the linear ultrasound transducer (indicated by the arrow in the figure) are electronically connected to the ultrasound scanner; the radio-frequency signal output is transmitted to the FEMMINA Platform by means of optic fiber. The set up is completed by a nanoparticle (NP) containing phantom (indicated in figure as "NP + agarose gel") immersed in a water tank (pointed by the respective arrow). US: Ultrasound.

The superficial distribution of FePt-IO and IO nanocrystals on a single SiNS is proportional to its diameter and was 90 ± 20, 140 ± 30 and 170 ± 30 NPs per 160, 330 and 660 nm SiNS respectively, and regardless of the specific magnetic coating[49]. The total number of superparamagnetic nanocrystals per mL $N_{nanocrystal/mL}$ in the NPCA-containing gel could be calculated at a given SiNS diameter as

$$N_{nanocrystal/mL} = N_{nanocrystal/SiNS_{Xnm}} \times (N_{NPCA_{Xnm}})/mL \quad (1)$$

where $N_{nanocrystal/SiNS_{Xnm}}$ is the number of nanocrystals adherent to a single SiNS with a given "X" diameter (X corresponding to 160, 330 or 660 nm), and $N_{NPCA_{Xnm}}/mL$ is the concentration of NPCA, with a given diameter of the SiNS, expressed in number of NPs per milliliter[49].

Magnetic measurements and nuclear magnetic resonance relaxometry

Magnetic properties were evaluated on Silica-based magnetic NPs in agarose gel using a quantum design superconducting quantum interference device (SQUID) MPMS-XL7 magnetometer[38].

The nuclear magnetic resonance (NMR) measurements were performed at room temperature by using a Bruker-MLS 200 NMR-FT spectrometer and a Tecmag-Apollo FT-NMR spectrometer both equipped with an electromagnet. The nuclear relaxation times were evaluated at frequencies of 12.5, 23 and 60 MHz. In order to eliminate the spin-diffusion effect in a non-homogeneous magnetic field, we used the Carr-Purcell-Meiboon-Gill (CPMG) pulse sequence for T_2 measurement and the saturation-recovery sequence for T_1.

The contrast efficiency of the MRI contrast agents is provided by the relaxivities $r_{1,2}$ defined as[50]:

$$r_i = [(1/Ti)_{meas}-(1/Ti)_{dia}]/c \quad i = 1, 2 \quad (2)$$

where $(1/T_i)_{meas}$ is the value measured on the sample with a concentration c of the magnetic center (*i.e.*, the iron content in IO and FePt-IO dimers), and $(1/T_i)_{dia}$ is the nuclear relaxation rate of the diamagnetic host solution. In our case, the different SiNSs (160, 330 and 660 nm in diameter) both covered and not-covered by magnetic NPs were dispersed in agarose gel.

US signal acquisition

US signals were acquired by means of an experimental set-up illustrated in Figure 2. A commercial echographic system consisting of a digital echograph (Megas GPX, Esaote Spa, Florence Italy) equipped with low frequency linear probe (LA532, Esaote Spa) was linked by means of an optical fiber (1Gb/s) to a prototype platform for acquisition of "raw" RF signal digitized at 40 MHz, 16 bit (FEMMINA system, ELEN Spa, Florence, Italy)[51].

The US transducer was mounted on the motorized mechanism of an infusion pump (KDS 100, KD Scientific Inc., Holliston, MA) in order to perform automatic and repeatable phantom scanning. Each sample was located in a fixed support at the bottom of a pure water tank. The US probe, partially immersed in water, was positioned perpendicular to the sample surface at such a distance that transducer focus (set to 2 cm) was located half-way through NP-containing gel depth. Echographic parameters were set to the following values: power of the transmitted signal = 50%, mechanical index (MI) = 0.5, gain = 0, time gain compensation = linear (1dB/cm). Frequency parameter was varied in three successive steps from 2.5 MHz to 4.5 MHz with a frequency step of 1 MH.

For each Eppendorf tube, at each employed US frequency, 850 frames were recorded. The frames were acquired at 12 frame per second (fps) with a constant speed of 12.5 mm/min. Echographic image were composed by raw data acquired with 180 tracks × 2500 points/track.

US signal analysis

For each sample scansion, raw RF frames were off-line processed with Fortezza software (Elen Spa, Florence, Italy) to obtain time dependent RF signal amplitude. Each RF signal was high-pass filtered and, then, the absolute value was calculated in order to identify the ultrasound backscatter amplitude. A rectangular region of interest (ROI) of 25 tracks × 360 points/tracks (9000 total points) was set manually over the central zone of the echographic image, in which the algorithm could calculate the average intensity value of backscattered signal, without boundary effect bias. From the total 850 mean backscatter values only the 300 central frames were considered, in which the ROI remained enough homogeneously far from sample edges.

RESULTS

Preliminarily to further experimental analyses, estima-

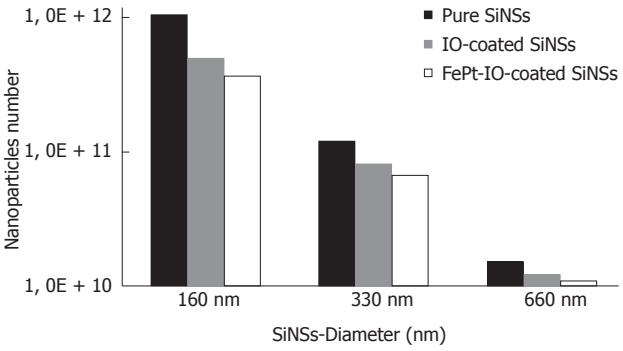

Figure 3 Estimation of nanoparticles number in 5 mg of nanoparticle contrast agents as a function of silica nanospheres diameter. SiNSs: Silica nanospheres; Pure: Uncoated SiNSs; FePt-IO: Ferrum platinum-iron oxide; IO: Iron oxide.

tions of NPCAs number are displayed in Figure 3, in which could be seen how the number of NPCAs varies between 1010 and 1012 NPs/mL. The number of NPCA was maximum for pure silica samples and decreases for IO and FePt-IO coated SiNS, proportionally to the weight of the two materials.

The SQUID measurements show superparamagnetism of the analyzed nanoparticles, with a blocking temperature (T_B) ranging from about 140 K to 154 K, presenting an arising trend with the increasing of SiNS diameter[38].

To check the efficacy of the synthesized nanocomposites as MRI contrast agents, proton relaxivity measurements were performed at three radio frequency (RF) frequencies: 12.5, 23 and 60 MHZ. In Figure 4 the r_1 and r_2 values measured for the different silica host nanospheres covered by IO (Figure 4A) or FePt-IO (Figure 4B) nanoparticles are reported as a function of the measuring proton NMR frequency. As the ratio r_2/r_1 is greater than 2, all the synthesized systems can be classified as good T_2-relaxing systems. In particular, for a T_2 contrast agent, a higher r_2/r_1 ratio has a better contrast efficacy[52]. Noticeably, for each employed RF frequency and SiNS-core diameter, the r_2/r_1 ratios of FePt-IO coated SiNSs are higher than those of IO coated SiNSs, indicating that Si@FePt-IO NPs are more efficiently as MRI negative contrast agents with respect to Si@IO NPs. For example at 23 MHz the r_2/r_1 ratio of FePt-IO coated SiNSs are 3-, 5- and 7-fold higher than those of IO coated SiNSs with 160, 240 and 330 nm of diameter, respectively.

Sample images of the US backscatter obtained at the lowest and highest employed frequency (2.5 MHz and 4.5 MHz, respectively) using 5 mg of pure, FePt-IO-coated and IO-coated SiNSs with a 660 nm SiNS core are reported in Figure 5. All the NPCA-containing samples produced a visible image enhancement (Figure 5A, F) compared to the pure agarose gel, that was essentially transparent to ultrasound (Figure 5G).

Based on qualitative investigations, the images obtained from phantoms containing pure SiNSs presented the strongest contrast power for each considered frequency (Figure 5A, D). The images obtained from FePt-

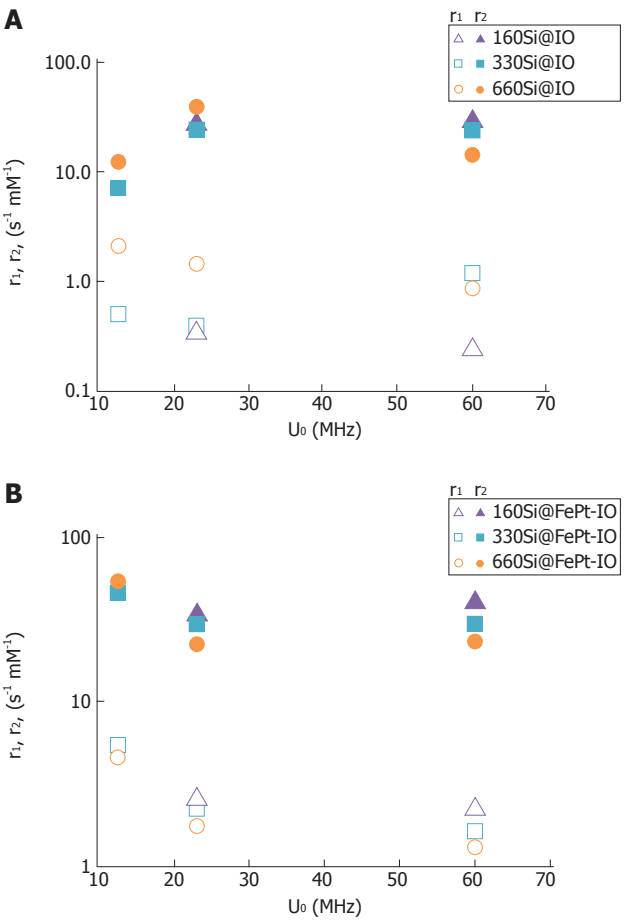

Figure 4 Longitudinal r1 (open symbols) and transverse r2 (full symbols) nuclear relaxitivities of different silica nanospheres. A: Silica nanospheres covered by IO; B: Silica nanospheres covered by FePt-IO nanoparticles. IO: Iron oxide; FePt-IO: Ferrum platinum-iron oxide.

IO-coated SiNSs containing phantoms (Figure 5B, E) showed a lower brightness and an image enhancement qualitatively analogous but less uniform than those of pure SiNSs. Even more markedly compared to FePt-IO-coated SiNSs, IO-coated SiNSs showed lowered brightness and less uniform image enhancement (Figure 5C, F).

These observations were confirmed by the quantitative results of a frame-by-frame analysis of the image backscatter intensity, evaluated in dB in order to appreciate even the smallest differences between the resulting values. As shown in Figure 6, 660 nm pure SiNSs showed the strongest US backscatter intensity for every US frequency employed whereas the lowest values was observed for 660 nm IO coated SiNSs. Moreover, our results proved how the image backscatter was raising with increasing insonification frequency. A similar image backscatter trend to that of 660 nm SiNS-based NPCAs has been observed for the other SiNS diameters.

Pure, IO-coated and FePt-IO-coated SiNSs determined a specific image enhancement behavior as function of different NPCA sizes (Figure 7, "zero" diameter was represented by the pure agarose sample) and type of magnetic coating; in order to focus these two vari-

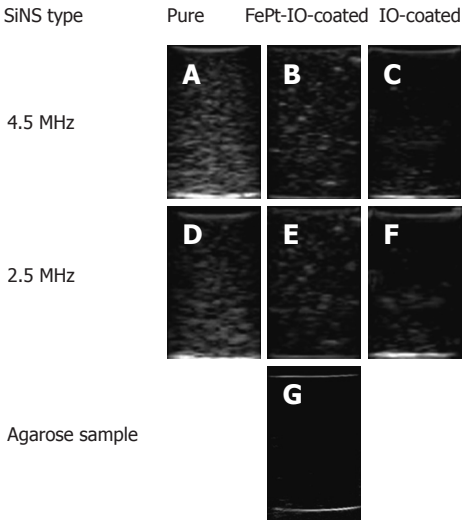

Figure 5 Examples of ultrasound image backscatter determined by pure and nanocomposite (with either ferrum platinum-iron oxide or iron oxide) 660 nm silica nanospheres at maximum and minimum used insonification frequency. A: Pure SiNSs, 4.5 MHz; B: FePt-IO-coated SiNSs, 4.5 MHz; C: IO-coated SiNSs, 4.5 MHz; D: Pure SiNSs, 2.5 MHz; E: FePt-IO-coated SiNSs, 2.5 MHz; F: IO-coated SiNSs, 2.5 MHz; G: Pure agarose gel. SiNSs: Silica nanospheres; Pure: Uncoated SiNSs; FePt-IO: Ferrum platinum-iron oxide; IO: Iron oxide.

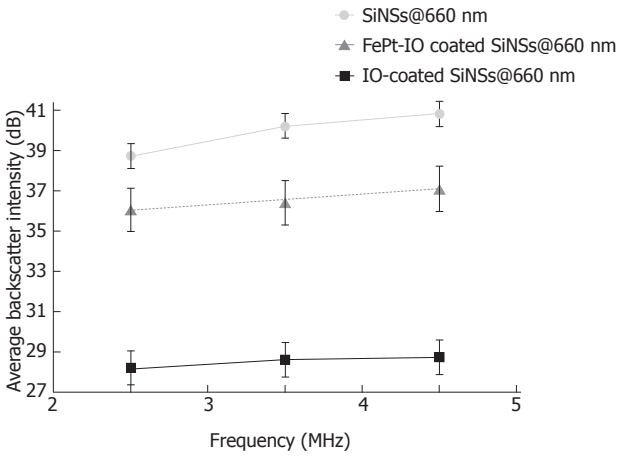

Figure 6 Average backscatter intensity for the three different types of nanoparticle contrast agents at 660 nm silica nanospheres diameter as a function of the frequency employed. Backscatter values are expressed in dB (values are averaged over 300 frames and error bars represent the standard deviations). **SiNSs**: Silica nanospheres; FePt-IO: Ferrum platinum-iron oxide; IO: Iron oxide.

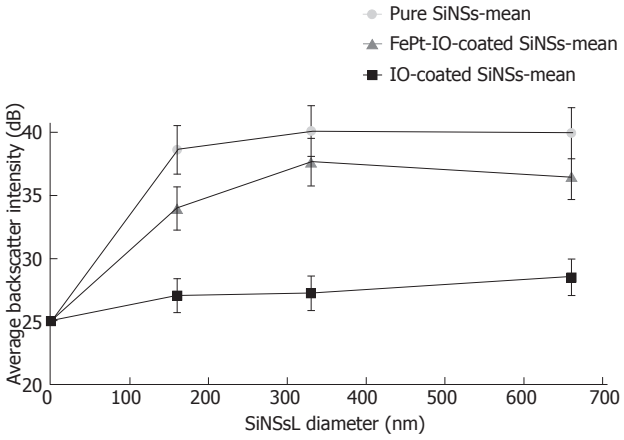

Figure 7 Mean average backscatter intensity for the three different types of nanoparticle contrast agents at each considered silica nanospheres diameter. Backscatter values are expressed in dB. 0-control point is obtained from pure agarose gel phantom measurements. Each curve represents the mean value of the acoustical response for a specific nanoparticle contrast agents over the entire low frequency range (2.5-4.5 MHz). SiNSs: Silica nanospheres; Pure: Uncoated SiNSs; FePt-IO: Ferrum platinum-iron oxide; IO: Iron oxide.

ables, the frequency-depending curves obtained for each insonification value (2.5, 3.5, 4.5 MHz) were averaged and mean backscatter values were plotted. For the investigated NPCA concentration, the presence of magnetic coating reduced the backscatter intensity compared to pure SiNSs and this reduction was more marked when SiNSs were coated with IO.

The acoustic signal response obtained using pure SiNSs, FePt-IO-coated SiNSs and IO-coated SiNSs at every considered US frequency and SiNS diameter was detailed in Figure 8. For pure SiNSs (Figure 8A) it is possible to note a peak of US backscatter in correspondence of 330 nm for the highest considered frequencies (3.5 and 4.5 MHz) whereas at 2.5 MHz the backscatter peak is modestly shifted to 660 nm. A similar behavior was observed for the FePt-IO-coated SiNSs (Figure 8B) but in a lower range of backscatter intensity values and a tendency to a more pronounced peak at 330 nm, decreasing towards SiNS diameter of 660 nm. Conversely, IO-coated SiNSs (Figure 8C) presented lower ranges of backscatter intensity values compared to the other investigated NPCAs and the value of US frequency employed had little influence on their acoustic response. Moreover, each frequency-dependent curve of IO-coated SiNSs was characterized by a raising trend for increasing SiNSs-diameter. In facts, the highest brightness value was observed at 660 nm.

DISCUSSION

Recent reports have highlighted the importance of developing novel nanosized contrast agents for multimodal molecular imaging[16,18]. In the present work, we investigated the low-frequency acoustic response of two of these novel NPCAs, made of SiNSs of different diameters coated by either IO or FePt-IO nanocrystals.

Magnetically-coated SiNSs at very low volume concentration (5 mg/mL) were insonified with low-frequency US pulses (range 2.5-4.5 MHz) and the results were compared with those of pure SiNSs.

Since previous publications demonstrated the effective signal enhancement at 5 mg/mL of SiNS[38,40] with a high level of biocompatibility[39], we defined the latter as the concentration tested, in favor of an overall higher systemic tolerance and safer cytotoxicity profile. Additionally, the explored SiNS diameter range was chosen taking into account that smaller particles can be hardly

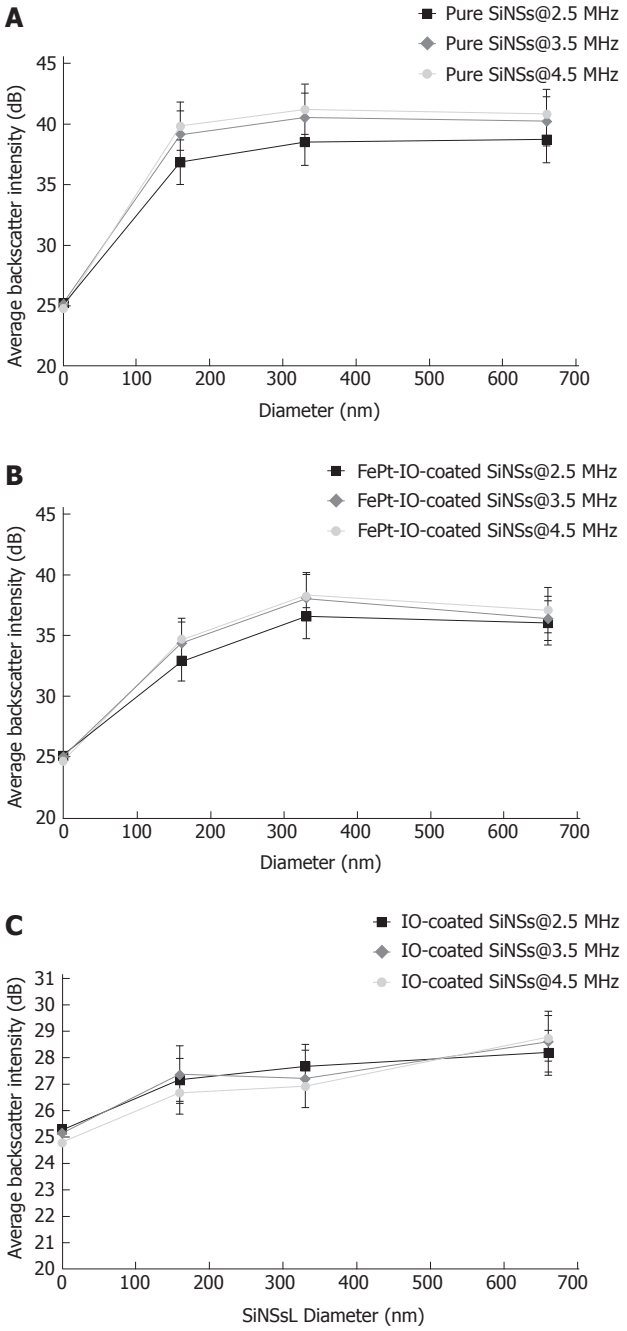

Figure 8 Average backscatter intensity as a function of silica nanospheres diameter for pure silica nanospheres. A: Pure SiNS; B: FePt-IO coated-SiNS; C: IO-coated SiNSs, at the three investigated ultrasound frequencies. Values of average backscatter intensity are expressed in dB in order to better emphasize lowest values. 0-control point value is obtained from pure agarose gel sample. SiNSs: Silica nanospheres; Pure: Uncoated SiNSs; FePt-IO: Ferrum platinum-iron oxide; IO: Iron oxide.

detected with diagnostic US pulses (unless using very high doses) and, if smaller than 50 nm, they can also distribute nonspecifically throughout the human body by passing through intercellular openings of normal vessel walls. On the other hand, bigger particles are rapidly sequestrated by the reticuloendothelial system, so being prevented from reaching the target site in a suitable concentration and, moreover, if their size exceeds that of tumor endothelium pores (780 nm) they will be also confined to the intravascular space, without the chance of extravasating and reaching target cells located beyond vessel walls[53,54].

Regardless the employed US frequency and the considered NPCA diameter, pure SiNSs present the strongest values in terms of backscatter amplitude (Figure 8). Reasons for the overall lower measured backscatter of the nanocomposite systems can be associated to various factors. Firstly, the addition of magnetic NPs causes a decrease in the US backscatter intensity reducing the concentration values in terms of NPCA number dispersed in 1 mL of agarose gel because of the increased NPCA size (Figure 3). Furthermore, adding the magnetic NP coating on SiNS surface alters its morphology in a significant and complex manner, that increases its roughness further affecting the related ultrasound backscatter pattern. The latter cause, in particular, can explain the difference in amplitude range between the two nanocomposite systems. In fact, despite the number of IO-coated SiNSs in 5 mg was larger compared to FePt-IO-coated SiNSs (because of the difference in the mass density of each particle component), IO-coated SiNSs evidenced the lowest backscatter intensity values.

The maximum brightness value for the two highest frequencies (3.5 and 4.5 MHZ) is reached for 330 nm SiNSs, wich represents also a particularly useful size for tumor targeting purposes. FePt-IO-coated SiNSs acoustical behavior followed a similar trend for every combination of NPCA diameter and scanning US frequency, with slightly lower intensities and a tendency to a more marked peak at 330 nm. Instead, particle size-dependent image backscatter behavior evidenced by IO-coated SiNSs proved how image brightness intensity became significant for larger dimensions of SiNSs (660 nm of diameter).

Moreover, we reported how US frequency affected the backscatter intensity; higher values were determined by higher frequency levels, for any given SiNS diameter. Frequency-dependent image enhancement was particularly evident for pure SiNS and became progressively less remarkable for FePt-IO coated and IO-coated SiNSs, respectively. For the latter type of NPCA the effect of increasing US frequency level on image backscatter is almost negligible.

These observations are in agreement with other results we have recently published, identifying the coating of SiNS core with FePt-IO as the best solution to realize an efficient ultrasound CAs at higher frequencies[38]. Moreover, based on the relaxometry results, the FePt-IO coated SiNSs have a better contrast efficacy as MRI negative contrast agents with respect to IO coated SiNSs, showing higher r_2/r_1 ratios. In conclusion, the MRI detectability, together with a good US contrast enhancement ability (even at low diagnostic frequencies, as evidenced in this study), make the FePt-IO coated SINSs as a novel promising NPCAs suitable for dual-mode molecular imaging of deep organs through US and MRI techniques.

COMMENTS

Background

Multimodal molecular imaging is one of the most exciting and rapidly growing areas of science because of its undoubted potential for enhancing diagnostic outcome, especially in oncology. Each imaging technique has certain advantages as well as limitation and in many clinical applications two or more imaging modalities are frequently needed to discern possible pathological changes in tissue. In fact, multimodal imaging has great benefit for diagnosis and therapy if the strengths of each modality can be fully appreciated, while ameliorating the weakness of any individual one. However, a safe and cost effective clinical employment of multimodal imaging entails the development of novel multimodal contrast agents, detectable by multiple non invasive and non-ionizing techniques, such as ultrasound (US) and magnetic resonance imaging (MRI).

Research frontiers

The US/MRI dual-mode contrast agents are mostly based on the existing US contrast media, such as microbubbles for US imaging encapsulating or absorbing MRI contrast agents. Beyond microbubbles, nanosized contrast agents also attract considerable interest for dual-mode imaging as they offer several advantages due to their unique features including multifunctionality, large surface area, structural diversity, and long circulation time. In this study, the authors explored the potential novel nanosized contrast agents (NPCAs) based on silica nanospheres coated with superparamagnetic nanoparticle, made of iron-oxide (IO) or FePt-IO nanocrystal, for dual mode imaging employing US and MRI imaging.

Innovations and breakthroughs

Recent reports of the authors documented the feasibility and detectability of magnetically-coated silica nanospheres (SiNSs) on conventional echographic images obtained at an US frequency (10 MHz) which is usually employed in clinical routine for imaging of superficial targets on the body. In this work the authors extendend the experimental characterization of the echographic effectiveness of magnetically-coated SiNSs to more feasible diagnostic settings, represented by a lower diagnostic frequencies (from 2.5 to 4.5 MHz), more suitable for deep organs, identifying the FePt-IO as the best magnetic coating for realizing NPCAs suitable for US/MRI dual mode imaging at low US frequencies.

Applications

These results open new exciting perspectives for dual mode molecular imaging of deep tumors, identifying the FePt-IO coated SINSs as a novel promising NPCAs suitable for dual-mode US/MRI contrast imaging for the accurate and early detection of cancer cells located in internal organs.

Terminology

Dual- or multi-modality molecular imaging is the synergistic combination of two or more imaging techniques, made possible by multimodal probes. Recent advance in nanotechnology have driven the development of multimodal nanoparticles that combines two or more nanomaterials with different imaging capabilities with the potential to integrate various functionalities, simultaneously providing contrast for different imaging techniques.

Peer review

The authors investigated the acoustic response at low US frequencies of novel dual-mode NPCAs, detectable through both US and MRI imaging. Such NPCAs are made of SiNSs of different diameters coated with superparamagnetic nanoparticles (IO or FePt-IO nanocrystals). The study proved that FePt-IO was the best magnetic coating for realizing NPCAs suitable for US/MRI dual mode imaging having a good US contrast enhancement ability together with a satisfying MRI detectability. The results are interesting and may open new exciting perspectives for dual mode molecular imaging of deep organs.

REFERENCES

1 **Huang Y**, He S, Cao W, Cai K, Liang XJ. Biomedical nanomaterials for imaging-guided cancer therapy. *Nanoscale* 2012; **4**: 6135-6149 [PMID: 22929990 DOI: 10.1039/c2nr31715j]

2 **Casciaro S**. Theranostic applications: Non-ionizing cellular and molecular imaging through innovative nanosystems for early diagnosis and therapy. *World J Radiol* 2011; **3**: 249-255 [PMID: 22229079 DOI: 10.4329/wjr.v3.i10.49]

3 **Correas JM**, Bridal L, Lesavre A, Méjean A, Claudon M, Hélénon O. Ultrasound contrast agents: properties, principles of action, tolerance, and artifacts. *Eur Radiol* 2001; **11**: 1316-1328 [PMID: 11519538 DOI: 10.1007/s003300100940]

4 **Raisinghani A**, DeMaria AN. Physical principles of microbubble ultrasound contrast agents. *Am J Cardiol* 2002; **90**: 3J-7J [PMID: 12450583 DOI: 10.1016/S0002-9149(02)02858-8]

5 **Sun C**, Lee JS, Zhang M. Magnetic nanoparticles in MR imaging and drug delivery. *Adv Drug Deliv Rev* 2008; **60**: 1252-1265 [PMID: 18558452 DOI: 10.1016/j.addr.2008.03.018]

6 **Borden MA**, Zhang H, Gillies RJ, Dayton PA, Ferrara KW. A stimulus-responsive contrast agent for ultrasound molecular imaging. *Biomaterials* 2008; **29**: 597-606 [PMID: 17977595 DOI: 10.1016/j.biomaterials.2007.10.011]

7 **Tartis MS**, Kruse DE, Zheng H, Zhang H, Kheirolomoom A, Marik J, Ferrara KW. Dynamic microPET imaging of ultrasound contrast agents and lipid delivery. *J Control Release* 2008; **131**: 160-166 [PMID: 18718854 DOI: 10.1016/j.jconrel.2008.07.030]

8 **Cai W**, Chen X. Nanoplatforms for targeted molecular imaging in living subjects. *Small* 2007; **3**: 1840-1854 [PMID: 17943716 DOI: 10.1002/smll.200700351]

9 **Sundararajan S**, Tohno E, Kamma H, Ueno E, Minami M. Detection of intraductal component around invasive breast cancer using ultrasound: correlation with MRI and histopathological findings. *Radiat Med* 2006; **24**: 108-114 [PMID: 16715671 DOI: 10.1007/BF02493276]

10 **Tang AM**, Kacher DF, Lam EY, Brodsky M, Jolesz FA, Yang ES. Multi-modal imaging: simultaneous MRI and ultrasound imaging for carotid arteries visualization. *Conf Proc IEEE Eng Med Biol Soc* 2007; **2007**: 2603-2606 [PMID: 18002528 DOI: 10.1109/IEMBS.2007.4352862]

11 **John R**, Nguyen FT, Kolbeck KJ, Chaney EJ, Marjanovic M, Suslick KS, Boppart SA. Targeted multifunctional multimodal protein-shell microspheres as cancer imaging contrast agents. *Mol Imaging Biol* 2012; **14**: 17-24 [PMID: 21298354 DOI: 10.1007/s11307-011-0473-7]

12 **Rapoport N**, Nam KH, Gupta R, Gao Z, Mohan P, Payne A, Todd N, Liu X, Kim T, Shea J, Scaife C, Parker DL, Jeong EK, Kennedy AM. Ultrasound-mediated tumor imaging and nanotherapy using drug loaded, block copolymer stabilized perfluorocarbon nanoemulsions. *J Control Release* 2011; **153**: 4-15 [PMID: 21277919 DOI: 10.1016/j.jconrel.2011.01.022]

13 **Liu X**, Tao H, Yang K, Zhang S, Lee ST, Liu Z. Optimization of surface chemistry on single-walled carbon nanotubes for in vivo photothermal ablation of tumors. *Biomaterials* 2011; **32**: 144-151 [PMID: 20888630 DOI: 10.1016/j.biomaterials.2010.08.096]

14 **Liu Y**, Miyoshi H, Nakamura M. Nanomedicine for drug delivery and imaging: a promising avenue for cancer therapy and diagnosis using targeted functional nanoparticles. *Int J Cancer* 2007; **120**: 2527-2537 [PMID: 17390371 DOI: 10.1002/ijc.22709]

15 **Conversano F**, Franchini R, Lay-Ekuakille A, Casciaro S. In vitro evaluation and theoretical modeling of the dissolution behavior of a microbubble contrast agent for ultrasound imaging. *IEEE Sens J* 2012; **12**: 496-503 [DOI: 10.1109/JSEN.2011.2109707]

16 **Swierczewska M**, Lee S, Chen X. Inorganic nanoparticles for multimodal molecular imaging. *Mol Imaging* 2011; **10**: 3-16 [PMID: 21303611]

17 **Cho EC**, Glaus C, Chen J, Welch MJ, Xia Y. Inorganic nanoparticle-based contrast agents for molecular imaging. *Trends Mol Med* 2010; **16**: 561-573 [PMID: 21074494 DOI: 10.1016/j.molmed.2010.09.004]

18 **Hahn MA**, Singh AK, Sharma P, Brown SC, Moudgil BM. Nanoparticles as contrast agents for in vivo bioimaging: current status and future perspectives. *Anal Bioanal Chem* 2011; **399**: 3-27 [PMID: 20924568 DOI: 10.1007/s00216-010-4207-5]

19 **Conversano F**, Soloperto G, Greco A, Ragusa A, Casciaro E, Chiriacò F, Demitri C, Gigli G, Maffezzoli A, Casciaro S. Echographic detectability of optoacoustic signals from low-concentration PEG-coated gold nanorods. *Int J Nanomedi-*

cine 2012; **7**: 4373-4389 [PMID: 22927756 DOI: 10.2147/IJN.S33908]
20 **Selvan ST**, Tan TT, Yi DK, Jana NR. Functional and multifunctional nanoparticles for bioimaging and biosensing. *Langmuir* 2010; **26**: 11631-11641 [PMID: 19961213 DOI: 10.1021/la903512m]
21 **Yang J**, Gunn J, Dave SR, Zhang M, Wang YA, Gao X. Ultrasensitive detection and molecular imaging with magnetic nanoparticles. *Analyst* 2008; **133**: 154-160 [PMID: 18227935 DOI: 10.1039/b700091j]
22 **Gupta AK**, Gupta M. Synthesis and surface engineering of iron oxide nanoparticles for biomedical applications. *Biomaterials* 2005; **26**: 3995-4021 [PMID: 15626447 DOI: 10.1016/j.biomaterials.2004.10.012]
23 **Kievit FM**, Zhang M. Surface engineering of iron oxide nanoparticles for targeted cancer therapy. *Acc Chem Res* 2011; **44**: 853-862 [PMID: 21528865 DOI: 10.1021/ar2000277]
24 **Xie J**, Liu G, Eden HS, Ai H, Chen X. Surface-engineered magnetic nanoparticle platforms for cancer imaging and therapy. *Acc Chem Res* 2011; **44**: 883-892 [PMID: 21548618 DOI: 10.1021/ar200044b]
25 **Chen S**, Wang L, Duce SL, Brown S, Lee S, Melzer A, Cuschieri A, André P. Engineered biocompatible nanoparticles for in vivo imaging applications. *J Am Chem Soc* 2010; **132**: 15022-15029 [PMID: 20919679 DOI: 10.1021/ja106543j]
26 **Prabhu P**, Patravale V. The upcoming field of theranostic nanomedicine: an overview. *J Biomed Nanotechnol* 2012; **8**: 859-882 [PMID: 23029995 DOI: 10.1166/jbn.2012.1459]
27 **Dave SR**, Gao X. Monodisperse magnetic nanoparticles for biodetection, imaging, and drug delivery: a versatile and evolving technology. *Wiley Interdiscip Rev Nanomed Nanobiotechnol* 2009; **1**: 583-609 [PMID: 20049819 DOI: 10.1002/wnan.51]
28 **McCarthy JR**, Weissleder R. Multifunctional magnetic nanoparticles for targeted imaging and therapy. *Adv Drug Deliv Rev* 2008; **60**: 1241-1251 [PMID: 18508157 DOI: 10.1016/j.addr.2008.03.014]
29 **Xu C**, Sun S. Superparamagnetic nanoparticles as targeted probes for diagnostic and therapeutic applications. *Dalton Trans* 2009; **(29)** : 5583-5591 [PMID: 20449070 DOI: 10.1039/b900272n]
30 **Ho D**, Sun X, Sun S. Monodisperse magnetic nanoparticles for theranostic applications. *Acc Chem Res* 2011; **44**: 875-882 [PMID: 21661754 DOI: 10.1021/ar200090c]
31 **Lacroix LM**, Ho D, Sun S. Magnetic nanoparticles as both imaging probes and therapeutic agents. *Curr Top Med Chem* 2010; **10**: 1184-1197 [PMID: 20388109 DOI: 10.2174/156802610791384207]
32 **Lin MM**, Kim do K, El Haj AJ, Dobson J. Development of superparamagnetic iron oxide nanoparticles (SPIONS) for translation to clinical applications. *IEEE Trans Nanobioscience* 2008; **7**: 298-305 [PMID: 19203873 DOI: 10.1109/TNB.2008.2011864]
33 **Hariri G**, Wellons MS, Morris WH, Lukehart CM, Hallahan DE. Multifunctional FePt nanoparticles for radiation-guided targeting and imaging of cancer. *Ann Biomed Eng* 2011; **39**: 946-952 [PMID: 21132370 DOI: 10.1007/s10439-010-0219-8]
34 **Vivero-Escoto JL**, Huxford-Phillips RC, Lin W. Silica-based nanoprobes for biomedical imaging and theranostic applications. *Chem Soc Rev* 2012; **41**: 2673-2685 [PMID: 22234515 DOI: 10.1039/c2cs15229k]
35 **Tallury P**, Payton K, Santra S. Silica-based multimodal/multifunctional nanoparticles for bioimaging and biosensing applications. *Nanomedicine* (Lond) 2008; **3**: 579-592 [PMID: 18694319 DOI: 10.2217/17435889.3.4.579]
36 **Insin N**, Tracy JB, Lee H, Zimmer JP, Westervelt RM, Bawendi MG. Incorporation of iron oxide nanoparticles and quantum dots into silica microspheres. *ACS Nano* 2008; **2**: 197-202 [PMID: 19206619 DOI: 10.1021/nn700344x]
37 **Aslam M**, Fu L, Li S, Dravid VP. Silica encapsulation and magnetic properties of FePt nanoparticles. *J Colloid Interface Sci* 2005; **290**: 444-449 [PMID: 15935370 DOI: 10.1016/j.jcis.2005.04.050]
38 **Malvindi MA**, Greco A, Conversano F, Figuerola A, Corti M, Bonora M, Lascialfari A, Doumari HA, Moscardini M, Cingolani R, Gigli G, Casciaro S, Pellegrino T, Ragusa A. Magnetic/silica nanocomposites as dual-mode contrast agents for combined magnetic resonance imaging and ultrasonography. *Adv Func Materials* 2011; **21**: 2548-2555 [DOI: 10.1002/adfm.201100031]
39 **Chiriacò F**, Conversano F, Soloperto G, Casciaro E, Ragusa A, Sbenaglia EA, Dipaola L, Casciaro S. Epithelial cell biocompatibility of silica nanospheres for contrast-enhanced ultrasound molecular imaging. *JNanoR* 2013; **15**: 1779 [DOI: 10.1007/s11051-013-1779-y]
40 **Casciaro S**, Conversano F, Ragusa A, Malvindi MA, Franchini R, Greco A, Pellegrino T, Gigli G. Optimal enhancement configuration of silica nanoparticles for ultrasound imaging and automatic detection at conventional diagnostic frequencies. *Invest Radiol* 2010; **4**5: 715-724 [PMID: 20562708 DOI: 10.1097/RLI.0b013e3181e6f42f]
41 **Conversano F**, Greco A, Ragusa A, Lay-Ekuakille A, Casciaro S. Harmonic ultrasound imaging of nanosized contrast agents for multimodal molecular diagnoses. *IEEE Trans Instr Meas* 2012; **61**: 1848-1856 [DOI: 10.1109/TIM.2012.2192354]
42 **Casciaro S**, Soloperto G, Greco A, Casciaro E, Franchini R, Conversano F. Effectiveness of functionalized nanosystems for multimodal molecular sensing and imaging in medicine. *IEEE Sens J* 2013; **13**: 2305-2312 [DOI: 10.1109/JSEN.2013.2252164]
43 **Liang HD**, Blomley MJ. The role of ultrasound in molecular imaging. *Br J Radiol* 2003; **76** Spec No 2: S140-S150 [PMID: 15572336]
44 **Stöber W**, Fink A, Bohn E. Controlled growth of nonodisperse silica spheres in the micron size range. *J Colloid Interface Sci* 1968; **26**: 62-69 [DOI: 10.1016/0021-9797(68)90272-5]
45 **Sun S**, Zeng H. Size-controlled synthesis of magnetite nanoparticles. *J Am Chem Soc* 2002; **124**: 8204-8205 [PMID: 12105897 DOI: 10.1021/ja026501x]
46 **Figuerola A**, Fiore A, Di Corato R, Falqui A, Giannini C, Micotti E, Lascialfari A, Corti M, Cingolani R, Pellegrino T, Cozzoli PD, Manna L. One-pot synthesis and characterization of size-controlled bimagnetic FePt-iron oxide heterodimer nanocrystals. *J Am Chem Soc* 2008; **130**: 1477-1487 [PMID: 18181628 DOI: 10.1021/ja078034v]
47 **Pellegrino T**, Manna L, Kudera S, Liedl T, Koktysh D, Rogach AL, Keller S, Rädler J, Natile G, Parak WJ. Hydrophobic nanocrystals coated with an amphiphilic polymer shell: a general route to water soluble nanocrystals. *Nanoletters* 2004; **4**: 703-707 [DOI: 10.1021/nl035172j]
48 **Di Corato R**, Quarta A, Piacenza P, Ragusa A, Figuerola A, Buonsanti R, Cingolani R, Manna L, Pellegrino T. Water solubilization of hydrophobic nanocrystals by means of poly(maleic anhydride-alt-1-octadecene). *J Mater Chem* 2008; **18**: 1991 [DOI: 10.1039/b717801h]
49 **Kircher MF**, Mahmood U, King RS, Weissleder R, Josephson L. A multimodal nanoparticle for preoperative magnetic resonance imaging and intraoperative optical brain tumor delineation. *Cancer Res* 2003; **63**: 8122-8125 [PMID: 14678964]
50 **Laurent S**, Vander Elst L, Roch A, Muller RN. Structure, synthesis and characterization of contrast agents for magnetic resonance molecular imaging. In: Carretta P, Lascialfari A. NMR-MRI, μ SR and Mossbauer Spectroscopies in Molecular Magnets. Milano: Springer-Verlag 2007: 71-88
51 **Masotti L**, Biagi E, Scabia M, Acquafresca A, Facchini R, Ricci A, Bini D. FEMMINA real-time, radio-frequency echo-signal equipment for testing novel investigation methods. *IEEE Trans Ultrason Ferroelectr Freq Control* 2006; **53**: 1783-1795 [PMID: 17036787 DOI: 10.1109/TUFFC.2006.111]
52 **Qin J**, Laurent S, Jo YS, Roch A, Mikhaylova M, Bhujwalla

ZM, Muller RN, Muhammed M. A High-Performance Magnetic Resonance Imaging T2 Contrast Agent. *Adv Mater* 2007; **19**: 1874-1878 [DOI: 10.1002/adma.200602326]

53 **Hobbs SK**, Monsky WL, Yuan F, Roberts WG, Griffith L, Torchilin VP, Jain RK. Regulation of transport pathways in tumor vessels: role of tumor type and microenvironment. *Proc Natl Acad Sci USA* 1998; **95**: 4607-4612 [PMID: 9539785 DOI: 10.1073/pnas.95.8.4607]

54 **Maeda H**, Wu J, Sawa T, Matsumura Y, Hori K. Tumor vascular permeability and the EPR effect in macromolecular therapeutics: a review. *J Control Release* 2000; **65**: 271-284 [PMID: 10699287 DOI: 10.1016/S0168-3659(99)00248-5]

P- Reviewers: Ferraioli G, Razek A, Shamsi K
S- Editor: Ma YJ **L- Editor**: A **E- Editor**: Liu XM

百世登

Baishideng®

Published by **Baishideng Publishing Group Co., Limited**
Flat C, 23/F., Lucky Plaza,
315-321 Lockhart Road, Wan Chai,
Hong Kong, China
Fax: +852-65557188
Telephone: +852-31779906
E-mail: bpgoffice@wjgnet.com
http://www.wjgnet.com